Available online at www.sciencedirect.com
SCIENCE DIRECT®
Physica E 26 (2005) 45–50
PHYSICA E
www.elsevier.com/locate/physe

Charged magneto-exciton states in semiconductor quantum dots

R.J. Warburton[a,*], B. Urbaszek[b], E.J. McGhee[a], C. Schulhauser[c], A. Högele[c], K. Karrai[c], B.D. Gerardot[d], P.M. Petroff[d]

[a]*Department of Physics, School of Engineering and Physical Sciences, Heriot-Watt University, Edinburgh EH14 4AS, UK*
[b]*Laboratoire de Physique de la Matière Condensée, LNMO-INSA-CNRS, 135 Avenue de Rangueil, 31077 Toulouse Cedex 4, France*
[c]*Center for NanoScience, Ludwig-Maximilians-Universität, Geschwister-Scholl-Platz 1, 80539 Munich, Germany*
[d]*Materials Department, University of California Santa Barbara, CA 93106, USA*

Available online 18 November 2004

Abstract

By embedding a layer of self-assembled quantum dots into a field-effect structure, we are able to control the exciton charge in a single dot. We present the results of photoluminescence experiments as a function of both charge and magnetic field. The results demonstrate a hierarchy of energy scales determined by quantization, the direct Coulomb interaction, the electron–electron exchange interaction, and the electron–hole exchange interaction. For excitons up to the triply charged exciton, the behavior can be understood from a model assuming discrete levels within the quantum dot. For the triply charged exciton, this is no longer the case. In a magnetic field, we discover a coherent interaction with the continuum states, the Landau levels associated with the wetting layer.

PACS: 73.21.La; 75.75.+a; 78.67.Hc

Keywords: Quantum dots; Excitons; Landau level

A self-assembled quantum dot has electronic levels separated by tens of meV as a result of the electronic quantization on a nanometer length scale [1]. The Coulomb energy between two electrons in such a quantum dot is also large, typically around 20 meV [1]. As a result, a self-assembled quantum dot exhibits a very pronounced Coulomb blockade [1]. This has been demonstrated even on an ensemble of self-assembled quantum dots as the inhomogeneous broadening can be sufficiently small that the Coulomb blockade is not smeared out [1,2]. In addition to the electronic Coulomb blockade, we have observed an excitonic Coulomb blockade by

*Corresponding author. Tel.: +44-1314518069; fax: +44-1314513136.
E-mail address: r.j.Warburton@hw.ac.uk (R.J. Warburton).

1386-9477/$ - see front matter © 2004 Elsevier B.V. All rights reserved.
doi:10.1016/j.physe.2004.08.020

measuring the photoluminescence (PL) from a single self-assembled quantum dot in a vertical tunneling structure [3]. At one voltage, the emission is completely dominated by one excitonic charge, with abrupt shifts in PL energy at special values of the voltage as the exciton charge changes by one quantum unit. We have recently extended these experiments to resonant excitation, detecting exciton formation in the transmission coefficient [4,5]. We present here a summary of the properties of charged excitons in a single self-assembled quantum dot.

The quantum dots for these experiments are produced by MBE in the Stranski–Krastanow growth mode of InAs on GaAs, increasing the ground state PL energy from 1.05 eV to about 1.3 eV with an annealing step during the overgrowth [6]. The dots are incorporated into a vertical tunneling structure; a back contact is connected to earth and the electric potential of the dots is changed via a voltage applied to a Schottky barrier on the surface. Details of the exact heterostructure can be found elsewhere [3,7]. Optical experiments are performed on a processed piece of wafer material using fiber-based confocal microscopes with the sample at 4.2 K. A magnetic field can be applied perpendicular to the quantum dot layer.

Fig. 1 shows the PL from a single quantum dot as a function of gate voltage, V_g, representing the PL intensity with a color scale. The exciton responsible for each emission line is marked. X^0 is the neutral exciton, X^{1-} the singly charged exciton, and so on. There is a large red-shift of the PL when the X exciton is transformed into X^{1-}. The origin of this is the Coulomb energy: the presence of the additional electron in the X^{1-} complex increases the renormalization of the emission energy. The ultimate origin of the red-shift is the smaller spatial extent of the hole wave function relative to the electron wave function [8]. While the red-shift of the ground state excitons in the PL is typically about 4 meV, the shifts of the excited state excitons can be much larger, ~20 meV, as in this case, the cancellation between the electron–electron and electron–hole interactions is less complete [7].

The X^{1-} extends over a larger region of voltage than the X^0 as a result of shell filling which is very

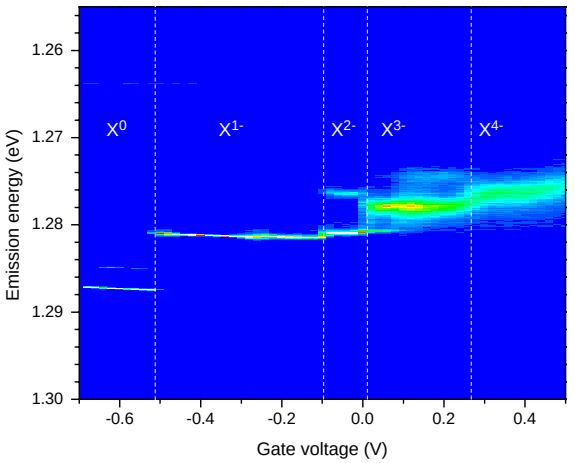

Fig. 1. Photoluminescence (PL) from a single quantum dot in a vertical tunneling structure as a function of voltage applied to the Schottky barrier on the sample surface. The PL intensity is represented with a color scale, with blue representing zero signal, with the signal rising as the color changes from green to yellow to red. The sample temperature was 4.2 K. The exciton state is labelled: X^0 denotes the neutral exciton, X^{1-} the singly charged exciton, and so on. The wetting layer loads with electrons around 0 V as revealed by the capacitance–voltage trace of the sample (not shown).

pronounced in self-assembled quantum dots. To form the X^{2-} electronic excited state, the p shell, must be occupied. As shown in Fig. 1, the X^{2-} is red-shifted with respect to the X^{1-}, again as a consequence of the Coulomb renormalization to the exciton energy, but in addition, the X^{2-} has a satellite at lower energy, as shown also in the PL spectrum in Fig. 2. The origin of the splitting is electron–electron exchange. After photon emission from the initial state with electron spin $S = \frac{1}{2}$, there are two possible final states, a triplet with $S = 1$ and a singlet with $S = 0$. These two states are split by $2X_{sp}$ where X_{sp} is the exchange energy between an s and a p electron, in complete analogy to the excited states of the He atom. The configuration diagrams for these states are shown in Fig. 3. The splitting for the dot in Fig. 2 is 4.2 meV, implying an exchange energy of $X_{sp} =$ 2.1 meV. A noticeable feature is that emission into the triplet is sharp with a line width below the resolution limit of our detection system (80 μeV), but the emission into the triplet is broad with a linewidth of typically 0.6 meV [3]. In both cases,

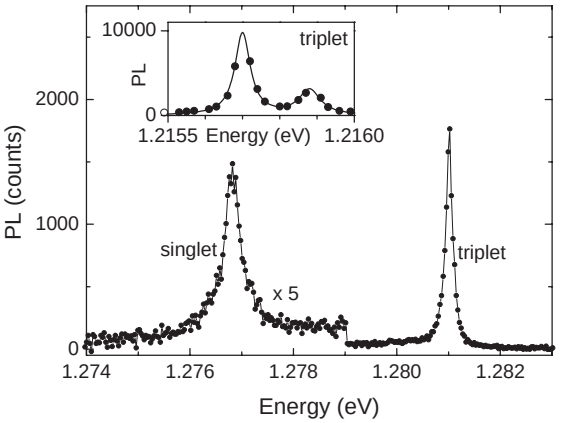

Fig. 2. The emission from X^{2-}, a doubly charged exciton. The PL consists of a sharp line and a broad satellite at low energy, corresponding to emission into the triplet and singlet final states, respectively. The emission into the triplet is itself split into two lines, as can be just made out in the main figure. The inset shows the triplet emission for a particularly low energy quantum dot where the splitting of the triplet is completely resolved. In the main figure, the solid line is a guide to the eye; in the inset, the solid line represents a fit to two Lorentzians.

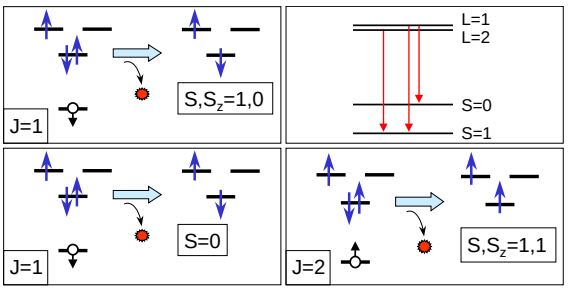

Fig. 3. Energy level diagrams showing the recombination of an X^{2-}. The electronic levels are the s level, and the p level with the $m=-1$ level shown to the left, the $m=+1$ level to the right. A spin-up electron is represented by $\uparrow$; a spin-down electron by $\downarrow$; and a hole with $\circ$ and associated spin $\left(\pm\frac{3}{2}\right)$. The large arrow connecting configurations denotes recombination. The total spin $J=1$ exciton has two possible recombination paths, one to the $S, S_z = 1, 0$ state and one to the $S=0$ state, both of which are equally likely. The $S, S_z = 1, 0$ and $S=0$ are represented in a simplified way; the states are in truth a sum (anti-sum) of the two possible configurations with $S_z = 0$. Conversely, the $J=2$ state has only one possible final state, the $S, S_z = 1, 1$ state. The $J=1$ and 2 states are split by the electron–hole exchange interaction, and the $S=1$ and $S=0$ states are split by the electron–electron exchange interaction ($2X_{sp}$), resulting in the energy level diagram shown. This energy level diagram accounts for the experimental spectrum shown in Fig. 2.

the final state is metastable. The p electron will ultimately relax into the s state. In the case of the singlet, relaxation does not require a spin flip, and relaxation occurs fast, in all likelihood by emission of an LO phonon. The fast relaxation broadens the PL, and the width can be used to measure the relaxation time, 1.1 ps. Conversely, the triplet can only relax by a process that dephases the spin, resulting in a slowed relaxation rate.

Emission into the X^{2-} triplet does not consist of a single line. Instead, it exhibits a fine structure, as shown in the inset to Fig. 2, a PL spectrum taken on a dot with stronger confinement than the dot used for the main part of the figure [9]. The origin of the fine structure, a splitting of 180 μeV, is the electron–hole exchange interaction. The isotropic part of the electron–hole exchange interaction splits the neutral exciton into two levels, the so-called dark exciton with total angular momentum $J=2$ at lower energy and the bright exciton with $J=1$ at higher energy. The splitting between the dark and bright excitons is typically hundreds of μeV in self-assembled quantum dots [10]. In the case of the X^{2-}, there are also two states, one with $J=1$ and one at lower energy with $J=2$; but now both states are bright. The reason for this is while the electron–hole exchange depends on the p shell electron, recombination depends on an s shell electron, as shown in Fig. 3. More precisely, both the $J=2$ and 1 states can recombine to the $S=1$ final state such that the splitting in the X^{2-} triplet emission arises from the splitting in the initial state. In this way, charging the dot with two additional electrons allows optical observation of a state which is normally dark. In principle, the $J=1$ state is split further by the anisotropic part of the electron–hole exchange interaction. For the ground state exciton, this splitting is a few tens of μeV and the optical transitions have characteristic linear and orthogonal polarizations [5].

Beyond the X^{2-}, a more positive bias induces the formation of the triply charged exciton, the X^{3-}. The X^{3-}, unlike the less highly charged excitons in this system, has two states close in energy, one with $S=1$ and the other with $S=0$. For a dot with high rotational symmetry, the two p electrons occupy the different p sub-shells in order to minimize the energy through electron

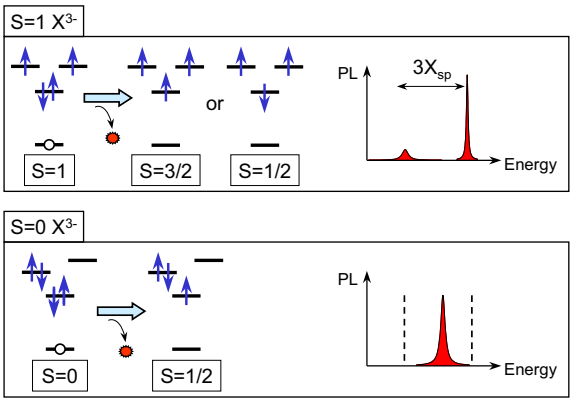

Fig. 4. The two low-energy X^{3-} configurations. The $S=1$ configuration has two possible final states, with $S=\frac{1}{2}$ and $\frac{3}{2}$. These two states are split by $3X_{sp}$ resulting in a splitting of the PL as shown schematically. The final state configurations are shown in a simplified way. The real configurations are admixtures of the configurations with the same spin and angular momentum quantum numbers. The $S=0$ configuration is favored when the degeneracy or near degeneracy of the p sub-shells is lifted. There is only one possible final state such that the PL lies between the exchange-split $S=1$ emission.

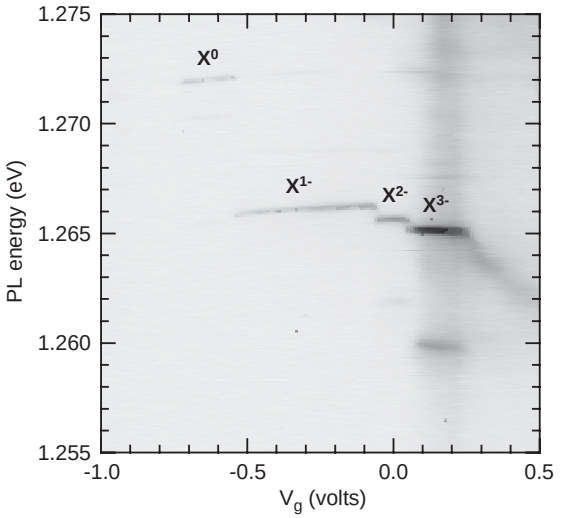

Fig. 5. Gray-scale plot of the PL from a single quantum dot vs bias at zero magnetic field. The dot shows a very clear $S=1$ X^{3-}. The wetting layer fills with electrons at 0.2 V in this case. The sample temperature is 4.2 K.

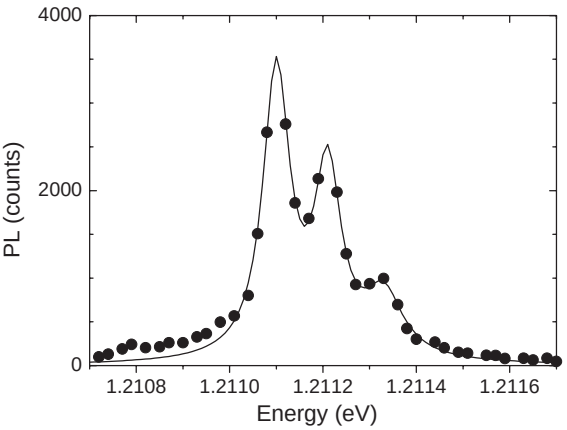

Fig. 6. Emission of an $S=1$ X^{3-} into the $S=\frac{3}{2}$ final state. The data are fitted to a sum of three Lorentzians. The observation of a triplet in the emission verifies that the spin of the initial state is $S=1$.

exchange. This configuration, shown in Fig. 4, has $S=1$. When the $S=1$ recombines, there are two possible final states, one with $S=\frac{3}{2}$ and one with $S=\frac{1}{2}$, which are split by $3X_{sp}$ by the electron–electron exchange interaction [3]. This is the spin state of the X^{3-} shown in the gray-scale plot in Fig. 5. Confirmation of the spin comes from spectroscopy of the higher energy emission, the emission into the $S=\frac{3}{2}$ final state, which consists of three closely spaced lines, typical of a spin-1 system, as a result of the electron–hole exchange in the $S=1$ initial state (see Fig. 6) [9]. The alternative X^{3-} state has $S=0$ and is favored when the symmetry is broken such that both p electrons occupy the lower p orbital (Fig. 4). Clearly, this configuration has lower energy than the $S=1$ configuration when the loss in exchange energy is more than compensated by the lower quantization energy. In this case, there is only one possible final state with $S=\frac{1}{2}$; the PL therefore consists of a single line in between the exchange-split lines from an $S=1$ X^{3-} (Fig. 4). We find that occupation of the wetting layer with electrons is sufficient to break the symmetry such that the $S=0$ X^{3-} is favored over the $S=1$ X^{3-}; an example of this behavior is shown in Fig. 1. Alternatively, for a highly symmetric dot, as in Figs. 5 and 7, a magnetic field can be used to lift the near-degeneracy of the two p sub-shells, forcing a change in the X^{3-} ground state from $S=1$ to 0, a process shown diagrammatically in Fig. 8.

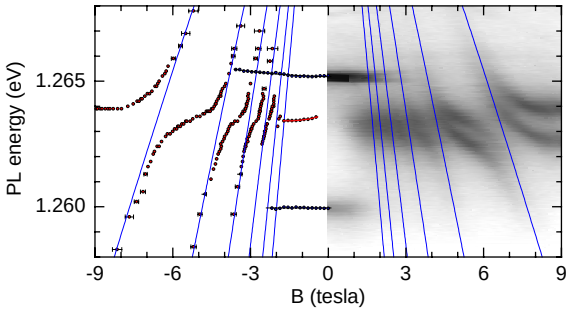

Fig. 7. X^{3-} emission vs magnetic field for the dot shown in Fig. 5. The data are represented with a gray-scale on the right, and as a fan diagram on the left. In the plot on the left, just one spin branch is plotted for simplicity. The exciton spin changes from $S = 1$ to 0 around 1 T. Thereafter, the emission shows a series of anti-crossings. The asymptotes are plotted and are close to linear functions of magnetic field, all extrapolating back to the same energy at zero magnetic field.

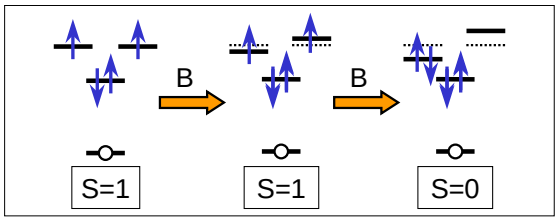

Fig. 8. The configuration diagrams for X^{3-} for a high symmetry dot. At zero magnetic field, the p sub-shells are degenerate such that the $S = 1$ X^{3-} has lower energy than the $S = 0$ X^{3-} because of electron exchange. As a magnetic field is applied, the degeneracy of the p sub-shells is lifted through the orbital Zeeman effect, and eventually the $S = 0$ X^{3-} has lower energy than the $S = 1$ X^{3-}. This transition occurs at about 1 T in the data in Fig. 7.

As the magnetic field is increased further, the PL from the $S = 0$ X^{3-} exhibits a remarkable series of anti-crossings [11] (Fig. 7). Conversely, the magnetic dispersion of the less highly charged excitons displays a diamagnetic shift and spin Zeeman splitting, behavior typical of a localized exciton [12]. Two factors point to a coupling to Landau levels in the case of the $S = 0$ X^{3-}. First, the intensity plotted at each PL energy is periodic in inverse magnetic field. Second, the asymptotes have a linear dependence on magnetic field, and all extrapolate back to the same energy (Fig. 7). The experiment therefore demonstrates that there is a

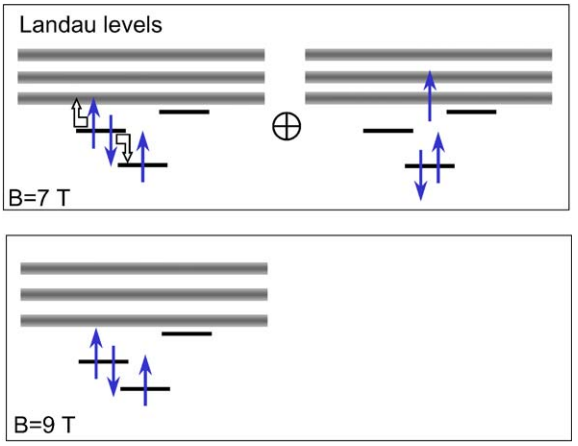

Fig. 9. The final state of the $S = 0$ X^{3-} at magnetic fields of 7 T and 9 T for the dot in Fig. 7. At 7 T there are two final states with the same quantum numbers and the same energy, one of which involves the lowest $n = 0$ Landau level, and the final state is therefore an admixture of the two. The hollow arrows show how the second configuration is related to the first by an Auger-like process. At 9 T, the Auger-like process provides insufficient energy to promote an electron into the $n = 0$ Landau level and the final state is therefore only weakly hybridized with the Landau levels.

coherent coupling to Landau levels. At first sight, this is a surprising result as the localized quantum dot levels lie well beneath the Landau levels associated with the wetting layer continuum.

The crucial pointer to the coherent hybridization with the Landau levels is the negative dispersion of the asymptotes, pointing to an interaction in the final state, after photon emission. After emission of a photon, the system is left with a vacancy in the s shell. If one of the p subshells is doubly occupied, then an Auger-like process can take place, with one p electron occupying the vacancy with the other forced to a higher energy level (Fig. 9). If the quantum dot had a confined d shell, this process would induce a hybridization with the d shell. In these experiments, the d shell is not bound, and instead the process induces a hybridization with continuum states. Each Landau level has a d-like part to the wave function, allowing each Landau level to be hybridized in turn as the magnetic field is increased. Essentially, there are two final states with the same quantum numbers, $|spp\rangle$ and

$|\mathrm{ssLL}(n)\rangle$, which anti-cross as the magnetic field is increased, causing the anti-crossings in the PL with the periodic behavior in inverse magnetic field. The magnitude of the anti-crossings can be accounted for by a direct calculation of the Coulomb matrix element [11]. In addition, we have discovered a relationship between the line width of the $S = 0$ X^{3-} at low field when the hybridization is largely incoherent, and the anti-crossing energies at high field, when the hybridization is coherent [11].

In conclusion, we have shown that it is possible to generate excitons of a specific charge in a single self-assembled quantum dot. The experiment exploits weak optical excitation and the strong Coulomb blockade in these quantum dots. The neutral, singly charged and doubly charged excitons have optical spectra which can be understood in the artificial atom model by considering just the confined electronic states in the quantum dot. Conversely, the spin-zero triply charged exciton cannot be understood within this picture. Instead, the final state after photon emission is hybridized with states which lie a quantization energy above the occupied p state. In our structures, this leads at high magnetic fields to a coherent hybridization with Landau levels.

This work was funded by EPSRC, The Royal Society and the DFG.

References

[1] M. Fricke, A. Lorke, J.P. Kotthaus, G. Medeiros-Ribeiro, P.M. Petroff, Euro. Phys. Lett. 36 (1996) 197.
[2] B.T. Miller, W. Hansen, S. Manus, R.J. Luyken, A. Lorke, J.P. Kotthaus, S. Huant, G. Medeiros-Ribeiro, P.M. Petroff, Phys. Rev. B 56 (1997) 1568.
[3] R.J. Warburton, C. Schäflein, D. Haft, A. Lorke, K. Karrai, J.M. Garcia, W. Schoenfeld, P.M. Petroff, Nature 405 (2000) 926.
[4] B. Alèn, F. Bickel, K. Karrai, R.J. Warburton, P.M. Petroff, Appl. Phys. Lett. 83 (2003) 2235.
[5] A. Högele, S. Seidel, M. Kroner, R.J. Warburton, K. Karrai, B.D. Gerardot, P.M. Petroff, unpublished.
[6] J.M. Garcia, G. Medeiros-Ribeiro, K. Schmidt, T. Ngo, J.L. Feng, A. Lorke, J. Kotthaus, P.M. Petroff, Appl. Phys. Lett. 71 (1997) 2014.
[7] R.J. Warburton, C.S. Dürr, K. Karrai, J.P. Kotthaus, G. Medeiros-Ribeiro, P.M. Petroff, Phys. Rev. Lett. 79 (1997) 5282.
[8] R.J. Warburton, B.T. Miller, C.S. Dürr, C. Bödefeld, K. Karrai, J.P. Kotthaus, G. Medeiros-Ribeiro, P.M. Petroff, S. Huant, Phys. Rev. B 58 (1998) 16221.
[9] B. Urbaszek, R.J. Warburton, K. Karrai, B.D. Gerardot, P.M. Petroff, J.M. Garcia, Phys. Rev. Lett. 90 (2003) 247403.
[10] M. Bayer, G. Ortner, O. Stern, A. Kuther, A.A. Gorbunov, A. Forchel, P. Hawrylak, S. Fafard, K. Hinzer, T.L. Reinecke, S.N. Walck, J.P. Reithmaier, F. Klopf, F. Schäfer, Phys. Rev. B 65 (2002) 195315.
[11] K. Karrai, R.J. Warburton, C. Schulhauser, A. Högele, B. Urbaszek, E.J. McGhee, A.O. Govorov, J.M. Garcia, B.D. Gerardot, P.M. Petroff, Nature 427 (2004) 135.
[12] C. Schulhauser, D. Haft, R.J. Warburton, K. Karrai, A.O. Govorov, A.V. Kalameitsev, A. Chaplik, W. Schoenfeld, J.M. Garcia, P.M. Petroff, Phys. Rev. B 65 (2002) 193303.